

# 3D Ly $\alpha$ radiation transfer. II. Fitting the Lyman break galaxy MS 1512–cB58 and implications for Ly $\alpha$ emission in high- $z$ starbursts

Daniel Schaerer<sup>1,2</sup>, Anne Verhamme<sup>1</sup>

<sup>1</sup> Observatoire de Genève, Université de Genève, 51, Ch. des Maillettes, CH–1290 Sauverny, Switzerland

<sup>2</sup> Laboratoire d’Astrophysique (UMR 5572), Observatoire Midi-Pyrénées, 14 Avenue E. Belin, F–31400 Toulouse, France

Received date; accepted date

## ABSTRACT

**Aims.** To understand the origin of the Ly $\alpha$  line profile of the prototypical Lyman break galaxy (LBG) MS 1512–cB58 and other similar objects. To attempt a consistent fit of Ly $\alpha$  and other UV properties of this galaxy. To understand the main physical parameter(s) responsible for the large variation of Ly $\alpha$  line strengths and profiles observed in LBGs.

**Methods.** Using our 3D Ly $\alpha$  radiation transfer code (Verhamme et al. 2006), we compute the radiation transfer of Ly $\alpha$  and UV continuum photons including dust. Observational constraints on the neutral gas (column density, kinematics, etc.) are taken from other analysis of this object.

**Results.** The observed Ly $\alpha$  profile of MS 1512–cB58 is reproduced for the first time taking radiation transfer and all observational constraints into account. The observed absorption profile is found to result naturally from the observed amount of dust and the relatively high HI column density  $N_{\text{H}}$ . Radiation transfer effects and suppression by dust transform a strong intrinsic Ly $\alpha$  emission with  $\text{EW}(\text{Ly}\alpha) \geq 60 \text{ \AA}$  into the observed faint superposed Ly $\alpha$  emission peak. We propose that the vast majority of LBGs have intrinsically  $\text{EW}(\text{Ly}\alpha) \sim 60\text{--}80 \text{ \AA}$  or larger, and that the main physical parameter responsible for the observed variety of Ly $\alpha$  strengths and profiles in LBGs is  $N_{\text{H}}$  and the accompanying variation of the dust content. Observed  $\text{EW}(\text{Ly}\alpha)$  distributions, Ly $\alpha$  luminosity functions, and related quantities must therefore be corrected for radiation transfer and dust effects. The implications from our scenario on the duty-cycle of Ly $\alpha$  emitters are also discussed.

**Key words.** Galaxies: starburst – Galaxies: ISM – Galaxies: high-redshift – Ultraviolet: galaxies – Radiative transfer – Line: profiles

## 1. Introduction

Discovered serendipitously by Yee et al. (1996), the Lyman Break Galaxy (LBG) MS 1512–cB58 (hereafter cB58) located at  $z \sim 2.73$  is strongly gravitationally magnified by the foreground cluster MS 1512+36. It is by far the best studied LBG, which has been observed at many wavelengths (see Baker et al. 2001, 2004; Bechtold et al. 1997; Ellingson et al. 1996; Frayer et al. 1997; Nakanishi et al. 1997; Pettini et al. 2002, 2000; Savaglio et al. 2002; Sawicki 2001; Teplitz et al. 2004, 2000). In particular, rest-frame UV (Pettini et al. 2002, 2000), optical (Teplitz et al. 2004, 2000), and radio (Baker et al. 2001, 2004) observations have allowed to draw a fairly global picture of this star-forming galaxy and its interstellar medium (ISM): it is young ( $\sim 50\text{--}300 \text{ Myr}$ ), massive ( $\sim 10^{10} M_{\odot}$ ), with a sub-solar metallicity ( $Z \sim 2/5 Z_{\odot}$ ), a star formation rate (SFR  $\sim 24 M_{\odot} \text{ yr}^{-1}$ ) typical of LBGs, and it is surrounded by outflowing material at  $V_{\text{exp}} \sim 250 \text{ km s}^{-1}$ .

Thanks to its apparent brightness the rest-UV spectra of this galaxy are of comparable quality as the best studied local starbursts. This has in particular made it possible to detect numerous stellar and interstellar (IS) lines, to study their kinematics, and to use them for detailed UV line fits to constrain its stellar content, age, star formation history etc. (e.g. de Mello et al. 2000; Ellingson et al. 1996; Pettini et al. 2000). Apart from its brightness, magnified by a factor  $\sim 30$  thanks to gravitational lensing (Seitz et al. 1998), the properties of cB58 are empirically found to be typical of LBGs (Shapley et al. 2003). More precisely, in

the sample of Shapley et al. (2003) cB58 is found in the quartile ( $\sim 25 \%$ ) of LBGs with the strongest Ly $\alpha$  absorption. As such a representative and given the quality and amount of observational data available, cB58 is of particular interest.

Our objectives are to examine if the observed Ly $\alpha$  line profile and strength of cB58 can be understood, and if one is able to obtain consistent diagnostics from the Ly $\alpha$  line and from the other UV and broad band features used in earlier papers. Such an attempt is carried out here for the first time with a Ly $\alpha$  radiation transfer code (Verhamme et al. 2006). Other LBGs with varying strengths of Ly $\alpha$  emission will be analysed in a subsequent paper (Verhamme et al. 2007). In particular we wish to elucidate what causes the broad Ly $\alpha$  absorption and very weak superposed Ly $\alpha$  emission in cB58 and in other LBGs showing similar Ly $\alpha$  spectra (cf. Shapley et al. 2003). Similarly we want to understand what physical parameter(s) distinguish the different subtypes of LBGs showing large variations especially in Ly $\alpha$ . Finally, fitting observed starburst spectra with detailed Ly $\alpha$  radiation transfer modeling should in general provide insight for the use of Ly $\alpha$  as a diagnostic in distant galaxies.

The remainder of the paper is structured as follows. The main observational properties of cB58 are summarised in Sect. 2. The principles of our simulations and fit method are described in Sect. 3. In Sect. 4 we discuss the implications from our results on the understanding of Ly $\alpha$  emission in LBGs, and on the properties of these galaxies. Our main conclusion are summarised in Sect. 6.

## 2. Observational constraints from cB58

The main properties of cB58 of relevance for the present paper are summarised in what follows.

### 2.1. Redshift and ISM outflow properties

Direct observations of photospheric lines by Pettini et al. (2002, 2000) assign the systemic redshift at  $z_{UV} = 2.7276^{+0.0001}_{-0.0003}$ . Teplitz et al. (2004) determine  $z_{HII} = 2.729 \pm 0.001$  from rest-frame optical emission lines (H $\alpha$ , [N II], [O III] and H $\beta$ ) of the counterarc ‘‘A2’’, in agreement with their earlier determination from the main image of cB58. The CO emission line determination by Baker et al. (2004) is  $z_{CO} = 2.7265^{+0.0004}_{-0.0005}$ .

The interstellar absorption lines and Ly $\alpha$  absorption are blueshifted by  $\sim 250 \text{ km s}^{-1}$  with respect to the galaxy redshift, determined by its photospheric lines. The small Ly $\alpha$  emission peak on top of the absorption (see e.g. Fig. 4) is redshifted by  $\sim 300 \text{ km s}^{-1}$  (Pettini et al. 2002). Both are evidence for large-scale outflowing medium around the star-forming galaxy.

Interestingly, and in contrast to the properties seen in the average LBG spectra of Shapley et al. (2003) and spectra of individual  $z \sim 3$  LBGs observed by Tapken et al. (2007), Ly $\alpha$  is redshifted in cB58 by a similar amount as the interstellar lines are blueshifted, instead of being redshifted by  $\sim +2 \times V_{\text{exp}}$  with respect to the stellar lines (or by  $\sim 3 \times V_{\text{exp}}$  from the IS lines). As discussed by Verhamme et al. (2006) the latter behaviour is naturally explained by a spherically symmetric expanding shell with constant velocity, where the emerging Ly $\alpha$  photons mostly originate from scattering on the backside of the shell where they gain redshift of  $\sim 2 \times V_{\text{exp}}$ . The smaller redshift of Ly $\alpha$  indicates already empirically a deviation from this simple symmetry. This will be substantiated below. How typical/frequent such velocity shifts are cannot be asserted from the available data, representing mostly stacked spectra. This will require many high quality spectra of individual LBGs. However, only the Ly $\alpha$  shape, not line shifts, is the criterion used to classify cB58 in the quartile with Ly $\alpha$  absorption.

The low ionisation ISM absorption lines yield consistently a velocity dispersion  $b = 70 \text{ km s}^{-1}$  (Pettini et al. 2002). The neutral hydrogen column density of the outflow is determined by Voigt fitting of the Ly $\alpha$  absorption wings;  $N_{\text{H}} = (7.0 \pm 1.5) \times 10^{20} \text{ cm}^{-2}$  and  $N_{\text{H}} = 6^{+1.4}_{-2} \times 10^{20} \text{ cm}^{-2}$  is obtained by Pettini et al. (2002) and Savaglio et al. (2002) respectively. Absorption profile line fitting shows that at least  $\sim 2/3$  of the low ionisation material is found at  $V = -265 \text{ km s}^{-1}$ , with a  $b$  parameter of  $70 \text{ km s}^{-1}$  (Pettini et al. 2002).

The outflow of cB58 is located well in front of the stars and covers them almost completely, since it absorbs almost all the UV light from the background stars. Indeed, Savaglio et al. (2002) find only a small residual mean flux above the zero level in the core of the Ly $\alpha$  absorption feature, whereas it is black for Pettini et al. (2002). Heckman et al. (2001) estimate an areal covering factor for optically thick gas of 98% from the residual intensity at the core of the C II  $\lambda 1335$  line.

### 2.2. Age and star-formation history of cB58

UV spectral fitting, including detailed stellar line profile fits, consistently indicate ages of  $\geq 20$ –100 Myr and favour constant star formation over this timescale (de Mello et al. 2000; Ellingson et al. 1996; Pettini et al. 2000). Such an age is also consistent with the observed stellar mass and star formation rate (Baker et al. 2004). Another independent argument in favour of

a young age is the underabundance of N and the Fe-peak elements in the ISM of cB58 (Pettini et al. 2002), giving the upper limit age  $\leq 300$  Myr, the timescale for the release of N from intermediate-mass stars.

### 2.3. Extinction/dust content

The precise amount of extinction in cB58 remains unclear. While Pettini et al. (2000) estimated  $E_s(B - V) = 0.29$  from their UV spectral fitting, and Teplitz et al. (2000) calculated  $E_g(B - V) = 0.27$  from the H $\alpha$ /H $\beta$  ratio, Baker et al. (2001) used four methods including a correction of the value derived from the Balmer decrement obtaining values from  $E_s(B - V) = 0.042$  to 0.236. Here  $E_s$  and  $E_g$  refer to the color excess of the stellar light and the nebular gas respectively, which are related by  $E_s(B - V) = 0.44 E_g(B - V)$  if the Calzetti law (Calzetti et al. 2000) applies. From this we conclude that  $E_g(B - V) \sim 0.10$ –0.54, and we adopt a mean value of  $E_g(B - V) \sim 0.3$  for simplicity.

### 2.4. Star formation rate, mass, and metallicity of cB58

The star formation rate estimated from the UV luminosity  $L_{1500}$  is  $\text{SFR}_{UV} \sim 40 M_{\odot} \text{ yr}^{-1}$  (Pettini et al. 2000) after correcting for reddening and gravitational magnification (assuming a magnification factor  $\mu = 30$ , cf. below). Adopting a lower extinction, based on the Balmer decrement, Baker et al. (2004) derive  $\text{SFR}_{H\alpha/H\beta} = 23.9 \pm 0.7 M_{\odot} \text{ yr}^{-1}$  from H $\alpha$ .

The velocity dispersion measured from nebular and CO emission lines are similar:  $\sigma_{\text{HII}} = 81 \text{ km s}^{-1}$  (Teplitz et al. 2000), and  $\sigma_{\text{CO}} = 74 \pm 18 \text{ km s}^{-1}$  (Baker et al. 2004). The dynamical mass deduced from these values, given the physical size of 2.4 kpc of the galaxy (Seitz et al. 1998), is  $M_{\text{dyn}} \sim 1. \times 10^{10} M_{\odot}$ . The mass of the gas deduced from the CO column density is  $M_{\text{gas}} = (6.6^{+5.8}_{-4.3}) \times 10^9 M_{\odot}$  (Baker et al. 2004).

The metallicity derived from the interstellar absorption lines and from the ionised region are compatible:  $Z_{\text{IS}} \sim 2/5 Z_{\odot}$  (Pettini et al. 2002) and  $Z_{\text{HII}} \sim 1/3 Z_{\odot}$  (Teplitz et al. 2000).

### 2.5. Gravitational lensing

Lensing reconstruction shows that the primary image of cB58, an arc whose spectrum will be used here, is magnified by 3.35–4 mag overall, i.e. a magnification factor  $\mu \sim 22$ –40 (Seitz et al. 1998). Approximately only a fraction 0.5–0.66 of the source is imaged into the cB58 arc according to Baker et al. (2004); Seitz et al. (1998). However, the fact that cB58 follows all the same scaling relations (among Ly $\alpha$  equivalent width, interstellar absorption line strengths, extinction etc. Shapley et al. (2003)) obeyed by unlensed LBGs, shows that the spectrum is not an unrepresentative slice of the galaxy.

## 3. Fitting the Ly $\alpha$ spectrum of cB58

### 3.1. Observations

We use the normalised rest-frame UV spectrum from Pettini et al. (2002), obtained with the Echelle Spectrograph and Imager (ESI) on the Keck telescope II at a resolution of  $58 \text{ km s}^{-1}$ , and kindly made available to us by Max Pettini. We have also examined the UVES spectrum taken with the VLT from Savaglio et al. (2002). Except for slight differences in the normalisation the spectra show a very good agreement (cf. Fig. 2). The former spectrum is used subsequently for our line profile fitting.

**Table 1.** Input parameters of the “standard” cB58 model for the radiation transfer code

$V_{\text{exp}} = V_{\text{front}}$	255 km s $^{-1}$
$V_{\text{back}}$	free
$N_{\text{H}}$	$7.0 \times 10^{20}$ cm $^{-2}$
$b$	70 km s $^{-1}$
$E_g(\text{B-V})$	0.3
$\text{FWHM}(\text{Ly}\alpha)$	80 km s $^{-1}$
$\text{EW}(\text{Ly}\alpha)$	free

### 3.2. Ly $\alpha$ plus UV continuum modeling

To fit the observations we use our 3D Monte Carlo (MC) radiation transfer code *MCLya* (Verhamme et al. 2006). The code solves the transfer of Ly $\alpha$  line and adjacent continuum photons including the detailed processes of Ly $\alpha$  line scattering, dust scattering and dust absorption.

For simplicity, and given empirical evidence in favour of a fairly simple geometry in  $z \sim 3$  Lyman Break Galaxies (hereafter LBG) discussed by Verhamme et al. (2006), we first adopted a simple “super-bubble” model to attempt fitting the observed Ly $\alpha$  line profile. The assumed “standard” geometry is that of an expanding, spherical, homogeneous, and isothermal shell of neutral hydrogen surrounding a central starburst emitting a UV continuum plus Ly $\alpha$  recombination line radiation from its associated H II region. The homogeneity and a covering factor near unity are also supported by the observations (cf. Sect. 2). Taking into account deviations from a constant expansion velocity is necessary to reproduce the observed Ly $\alpha$  profile of cB58, as already indicated from the empirical evidence discussed earlier.

#### 3.2.1. Radiation transfer modeling

The following geometries have been adopted: 1) a spherically symmetric expanding shell with velocity  $V_{\text{exp}}$ , 2) a foreground slab moving towards the observer with velocity  $V_{\text{front}} = V_{\text{exp}}$ , and 3) two parallel slabs with different velocities  $V_{\text{back}}$  and  $V_{\text{front}} = V_{\text{exp}}$  respectively to mimic a shell like geometry allowing for velocity variations between the front and the back of the shell. The value of  $V_{\text{exp}}$  is taken from the observations.  $V_{\text{back}}$  is a free parameter.

The other model parameters are: the velocity dispersion given by the Doppler parameter  $b$ , the H I column density  $N_{\text{H}}$ , and the dust absorption optical depth  $\tau_a$  at Ly $\alpha$  wavelength. We assume that dust and H I are uniformly mixed. As discussed in Verhamme et al. (2006),  $\tau_a$  relates to the usual extinction  $E(\text{B} - \text{V}) \approx (0.06 \dots 0.11) \tau_a$ , where the numerical coefficient covers attenuation/extinction laws of Calzetti et al. (2000), Seaton (1979) and similar. Here we assume  $E(\text{B} - \text{V}) = 0.1 \tau_a$ . The values for these parameters, summarised in Table 1, are taken from the observations of cB58 (Sect. 2). Note that we suppose that the color excess measured for the nebular gas is representative for the dust optical depth seen by the Ly $\alpha$  photons.

The spectrum of the central point source is described by the stellar continuum around Ly $\alpha$ , either a flat continuum or synthetic starburst spectra described below, and the nebular recombination line, described by its equivalent width  $\text{EW}(\text{Ly}\alpha)$  and full width at half maximum  $\text{FWHM}(\text{Ly}\alpha)$ . Although in principle the equivalent width of the intrinsic Ly $\alpha$  emission is determined by the stellar population, i.e. can be predicted by the synthetic spectra,  $\text{EW}(\text{Ly}\alpha)$  is kept as a free input parameter for the radiation transfer modeling. The resulting fit values will subsequently be compared to values expected from synthesis models to exam-

ine if consistent solutions can be obtained. The value for FWHM is taken from the observed H $\alpha$  line ( $\sigma_{\text{HII}}$ ).

For the spherical shell (1), the emergent spectrum is computed by integration over the entire volume. This assumes that the shell is unresolved and completely integrated within the spectroscopic aperture, which corresponds to  $\sim 2$  kpc (Seitz et al. 1998). For the slabs (2), the emergent spectra are computed taking the photons emitted within an opening angle of typically 60 degrees into account. The results depend little on the exact opening angle.

All models have been computed using the Monte Carlo (MC) radiation transfer code *MCLya* developed by Verhamme et al. (2006). The code treats the scattering of line and continuum photons in the Ly $\alpha$  line and the adjacent continuum, as well as scattering and absorption by dust. In practice one high statistics MC simulation is run for each set of parameters listed above assuming a constant (flat) input spectrum. By keeping trace of the relation between the input frequency bin of the photons and their emergent frequency, simulations for arbitrary input spectra can be generated a posteriori in an interactive manner. This avoids unnecessary transfer computations without resorting to any simplifying assumption. For comparison with the observations, the theoretical spectrum is finally convolved with a gaussian to the instrumental resolution.

Simulations for multi-slab geometries (3) have been computed by combining the results from a single slab MC computations in a numerical fashion, modifying appropriately the relative velocity shifts of the slabs and opening angles of the emerging radiation. This allows fast, interactive fitting, without resorting e.g. to approximate analytic fits (cf. Hansen and Oh 2006).

#### 3.2.2. Synthetic starburst spectra in the Ly $\alpha$ region

When spatially integrated galaxy spectra are considered, it is a priori necessary to include both stellar and nebular lines in fits of observed spectra. As the region around Ly $\alpha$  is generally not considered and not included or discussed in most evolutionary synthesis codes, we here briefly examine the behaviour of this spectral range. To do so we use the evolutionary synthesis models of Schaerer (2003) (hereafter S03) complemented by the recent models of Delgado et al. (2005) including high spectral resolution stellar atmospheres, kindly made available to us by Miguel Cerviño. Only the main ingredients of these model sets shall be summarised here.

The S03 models basically include simplified non-LTE model atmospheres for massive stars ( $> 20 M_{\odot}$ ), and LTE line blanketed Kurucz atmospheres otherwise. The Delgado et al. (2005) models include in particular theoretical high spectral resolution libraries, and all massive stars are treated with the plane parallel non-LTE blanketed TLUSTY code (Lanz and Hubeny 2003). In both cases the same stellar tracks and metallicities, summarised in S03, have been used. With respect to the Ly $\alpha$  region these models represent the most up-to-date computations. The only restriction is that these computations do not treat the stellar winds of the hottest stars, which leads to some modifications of the intrinsic Ly $\alpha$  line profile of these stars. However, unpublished test computations (Martins 2000) show that these effects are small or negligible compared to the underlying Ly $\alpha$  absorption from the bulk of B and A stars and compared to the expected nebular emission. This is also confirmed by Leitherer (2007).

In Fig. 1 we show the spectra predicted by these two synthesis over the spectral range centered on Ly $\alpha$ . The spectra, computed for instantaneous bursts with ages 0.1, 10, and 50 Myr at solar metallicity and for a Salpeter IMF with an up-

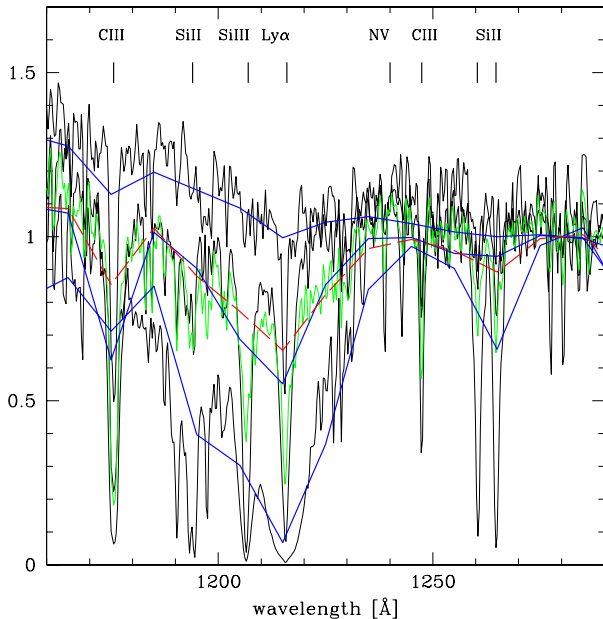


**Fig. 1.** Predicted stellar spectra around Ly $\alpha$  from the synthesis models of S03 (blue and red low-resolution curves), and the high-resolution models of (Delgado et al. 2005) in black and green. Computations for solar metallicity bursts of ages 0.1, 10, and 50 Myr are shown from top to bottom. The green line shows the equilibrium spectrum reached for constant star formation, as the red dashed line for the S03 model. All spectra are in  $F_\lambda$  units, normalised arbitrarily at 1280 Å. The main photospheric line identifications are indicated at the top (cf. text). Note the excellent overall agreement of the two independent models, allowing a reasonable description of the broad absorption around Ly $\alpha$ .

per mass cut-off of  $100 M_\odot$ , are normalised arbitrarily at 1280 Å. The high-resolution spectra allow the identification of the main (photospheric) spectral lines, which are the C III multiplet centered at 1175.6 Å, Si II multiplets at  $\lambda\lambda$  1193.3, 1194.5 and 1260.4, 1264.7, the Si III multiplet  $\lambda\lambda$  1206.5, 1207.5, and C III  $\lambda$  1247.4. The position of the N V multiplet  $\lambda\lambda$  1238.8, 1242.8 formed in the winds of early type stars (not included in the present models) is also indicated.

The temporal behaviour of the Ly $\alpha$  profile in a burst can be sketched as follows: for ages  $\leq 10$  Myr the Ly $\alpha$  absorption deepens but remains relatively narrow. At older ages, when stars with a lower ionisation degree in their atmospheres dominate, the Ly $\alpha$  becomes considerably stronger and broader. At  $> 50$  Myr, not shown here, the red wing remains broad, whereas the flux shortward of Ly $\alpha$  disappears very rapidly. For constant (ongoing) star formation the spectrum reaches quite shortly (over  $\geq 10$  Myr) an equilibrium with a Ly $\alpha$  line profile quite closely resembling that of a  $\sim 10$  Myr burst, as also shown in Fig. 1.

The shape of the red wing of Ly $\alpha$ , up to  $\sim 1240$  Å, provides a useful constraint on the age and star formation history of the starburst. For bursts with ages  $\gg 10$  Myr the width of the stellar Ly $\alpha$  absorption become so large, that a measurement of the shape of its red wing can already be distinctive, even without considering interstellar Ly $\alpha$  radiation transfer. For example, for the case of cB58 shown in Fig. 2 the observed Ly $\alpha$  wing is clearly less broad than the burst model at 50 Myr. Younger bursts

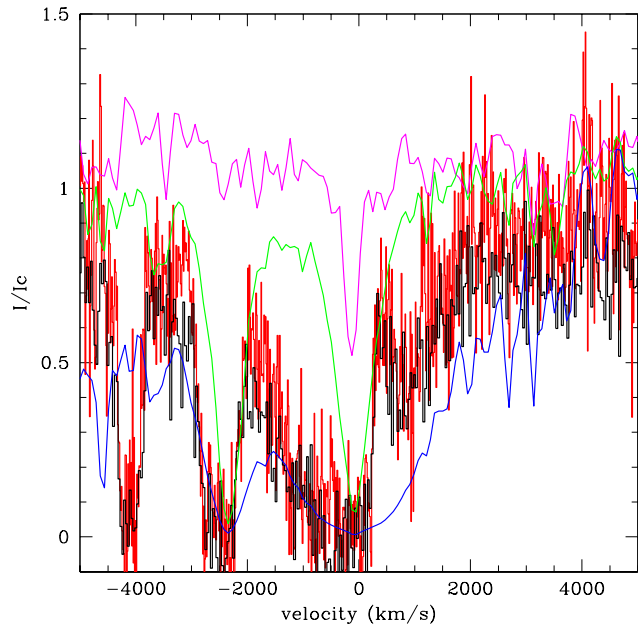


**Fig. 2.** Observed spectra of cB58 from Pettini et al. (2002) (black) and Savaglio et al. (2002) (red) compared to the high-resolution synthesis models of (Delgado et al. 2005) for solar metallicity bursts of ages 0.1, 10, and 50 Myr (in magenta, green and blue from top to bottom). Apart from small differences in the normalisation the two observed spectra are very consistent. The comparison with the models illustrates how the shape of the red wing of Ly $\alpha$  can be clearly used to exclude bursts of ages larger than 10–50 Myr.

or a more constant star formation history are therefore required. Of course, other UV spectral lines such as the well known Si IV and C IV lines, are sensitive to age and star formation history (cf. Leitherer et al. 1995).

As other parts of the UV spectrum (see e.g. Leitherer et al. 1999), the detailed integrated spectrum in the Ly $\alpha$  region depends also somewhat on metallicity (cf. Fig. 3). The main reason is the systematic shift of the average stellar effective temperature with metallicity for a given age. In consequence similar spectra of bursts can be obtained at different metallicities, provided some age shift is allowed. Despite the detailed metallicity differences, which can be accounted for by using the appropriate high resolution spectra, the overall behaviour of the shape of the Ly $\alpha$  profile remains quite independently of metallicity, as could be expected.

It is also reassuring to note the good overall agreement of the two independent synthesis models, allowing a reasonable description of the broad absorption around Ly $\alpha$  even with low-resolution spectra. In any case predictions from both synthesis models, as well as flat spectra, will be used below as input for the cB58 fits with the Ly $\alpha$  radiation transfer code.

The relative strengths of the stellar Ly $\alpha$  absorption and expected intrinsic nebular emission is illustrated in Fig. 3, where the predicted Ly $\alpha$  equivalent widths of these components are plotted as a function of time for the case of instantaneous bursts and for constant star formation, as well as for three different metallicities. The behaviour of these quantities is as expected from earlier computations at solar metallicity (Charlot and Fall 1993; Valls-Gabaud 1993). Decreasing metallicity increases the nebular emission and introduces a small age shift in Ly $\alpha$  absorp-

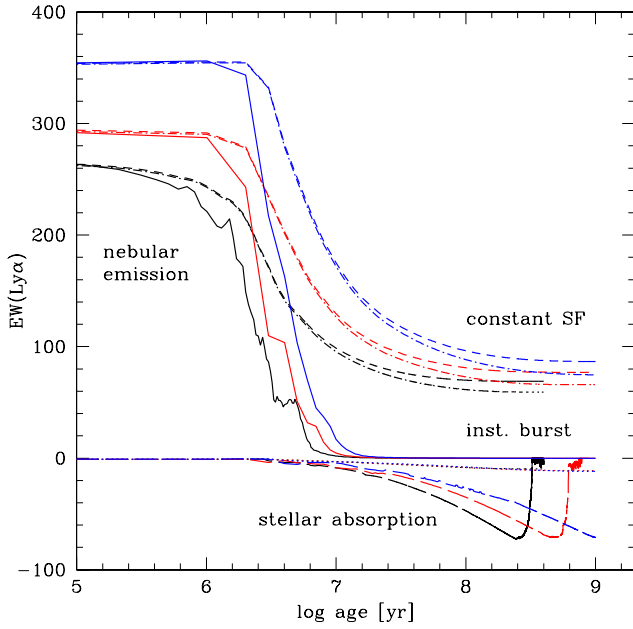


**Fig. 3.** Predicted Ly $\alpha$  equivalent widths of the nebular emission ( $EW(\text{Ly}\alpha) > 0$ ) and stellar absorption ( $EW(\text{Ly}\alpha) < 0$ ) for instantaneous bursts (solid and long-dashed lines) and models with constant star formation (short dashed, dotted, and dash-dotted). The long-dashed lines show the total EW (nebular + stellar) for constant star formation, the dotted lines the stellar absorption component. Three different metallicities,  $Z = 0.02$  (solar, black), 0.004 (red), and 0.0004 (blue) are shown.

tion. For constant star formation over  $\sim 20$ – $100$  Myr or more, one expects in particular  $EW(\text{Ly}\alpha) \sim 60$ – $100$  Å.

## 4. Results

We now discuss the simulated spectra assuming different geometries and their dependence on the input parameters.

### 4.1. Models for a constant velocity shell

The predicted Ly $\alpha$  line profile for a symmetric spherical shell with constant velocity, computed with the input parameters summarised in Table 1 and with  $EW(\text{Ly}\alpha) = 0, 10,$  and  $40$  Å is compared to the observed profile in Fig. 4. The input spectrum, here a flat continuum plus line, is also shown for illustration.

As expected from our earlier simulations (Verhamme et al. 2006), the global shape of the theoretic spectrum is similar to the observed one, consisting of a broad damped absorption plus a redshifted asymmetric emission line component, whose strength depends on the strength (EW) of the input line. The net absorption is due to dust absorption, since the case considered here is the integrated spectrum of a shell, where all scattered photons are observed. Scattering of photons out of the line of sight is therefore not possible, hence any net absorption must be due to dust. The superposed emission peak results from the radiation transfer of the photons from the original (input) emission line, which are scattered and absorbed, and are able to escape only thanks to their redshift acquired on the back of the shell.

Two main problems are immediately clear from Fig. 4. First the predicted width of the absorption is insufficient, and sec-

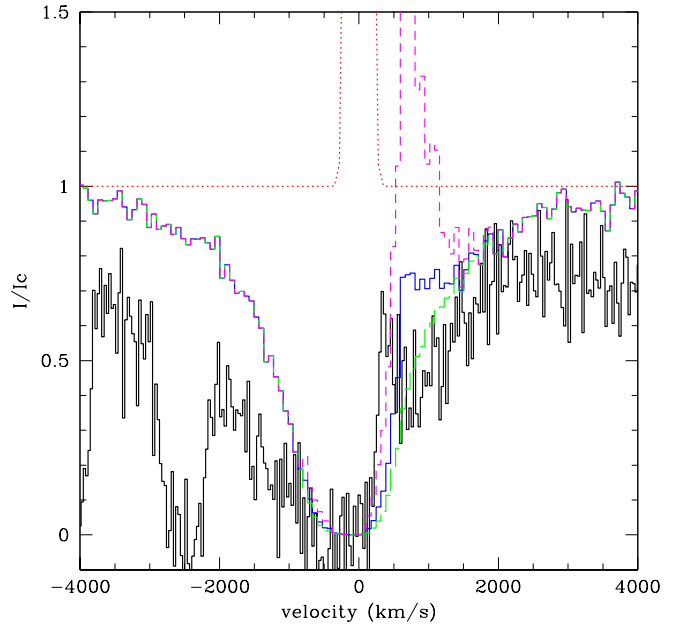


**Fig. 4.** Predicted Ly $\alpha$  line profile for a symmetric spherical shell with constant velocity, the input parameters summarised in Table 1, and  $EW(\text{Ly}\alpha) = 0, 10, 40$  Å (green, blue, magenta respectively). The input spectrum is the red dotted line. The observed spectrum of cB58 from Pettini et al. (2002) is shown in black.

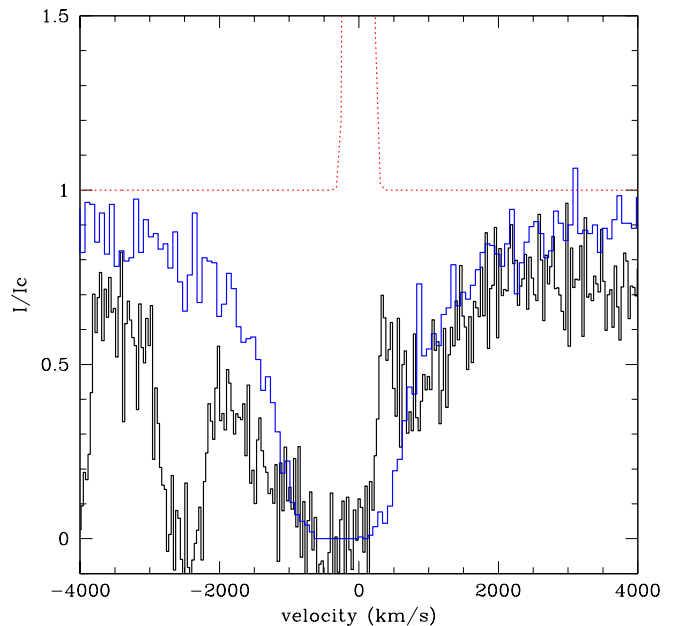


**Fig. 5.** Observed (black) and predicted Ly $\alpha$  line profile for the single foreground slab model (blue). The input spectrum, shown by the red dotted line has  $EW(\text{Ly}\alpha) = 40$  Å.

ond the position of the predicted Ly $\alpha$  emission peak is found at too high positive velocities. The first problem can be solved by increasing the column density of the shell. As already mentioned above, and first pointed out by Verhamme et al. (2006), an integrated shell geometry necessarily requires a larger  $N_H$  to reproduce a simple Voigt profile of the same width as a slab of

the same column density. The second discrepancy with the simple shell model could also be anticipated (cf. Sect. 2), since the redshifted peak of Ly $\alpha$  is expected at  $2 \times V_{\text{exp}}$ , whereas the observations show the peak around  $\sim 300 \text{ km s}^{-1}$ . As the velocity shift of the Ly $\alpha$  peak is a fairly generic feature of symmetric expanding shell models, it is clear that this discrepancy cannot be resolved by changes of the input parameters, such as  $N_{\text{H}}$ ,  $b$ ,  $E(\text{B}-\text{V})$ , etc. This has been confirmed by numerous model calculations.

Note also that this model allows only for a fairly weak intrinsic Ly $\alpha$  emission with  $\text{EW}(\text{Ly}\alpha) < 10 \text{ \AA}$ , much lower than the value expected from synthesis models for the star formation history derived for cB58 (cf. below).

#### 4.2. Single slab model

Given the difficulties with a simple shell model and the fact that the direct observational constraints on the outflow only relate to cold material in front of the UV source, one could ask the question whether a single moving foreground slab (without any backscattering source) could explain the observations. In other words this boils down to the question if the observed velocity shift of  $\sim 255 \text{ km s}^{-1}$  between stellar and interstellar absorption lines could be enough to allow for a partial transmission of the intrinsic Ly $\alpha$  line, such that it appears at velocities  $\geq 250 \text{ km s}^{-1}$ ? The simple answer obtained from many simulations is no. More precisely, with the observed column density,  $b$  parameter,  $E(\text{B}-\text{V})$ , and  $\text{FWHM}(\text{Ly}\alpha)$  the transmission of Ly $\alpha$  line photons emitted at line center ( $V = 0$ ) through a slab is negligible, and hence no line is formed on top of the broad absorption line profile, independently of the intrinsic Ly $\alpha$  equivalent width. This is shown in Fig. 5.

For enough line photons to escape through the slab the intrinsic emission line must be redshifted by  $> 200 \text{ km s}^{-1}$ , which is larger than the possible redshift of  $\sim 100 \text{ km s}^{-1}$  found by Teplitz et al. (2000) from 10 restframe optical nebular emission lines<sup>1</sup>. In any case, such a solution would require a large intrinsic Ly $\alpha$  equivalent width ( $\text{EW}(\text{Ly}\alpha) \gtrsim 40 \text{ \AA}$ ) in agreement with the results found below.

Hence the presence and position of the Ly $\alpha$  peak together with a relatively large HI column density testified by the damped absorption excludes most likely a pure foreground slab. To allow for the Ly $\alpha$  transmission, a receding background screen must be present so that the Ly $\alpha$  photons can gain an additional redshift by bouncing off the back, in a similar fashion as in the spherical shell. Such a situation will be simulated now.

#### 4.3. Models for two moving slabs

To attempt reproducing the observed Ly $\alpha$  emission component we now assume a geometry with two parallel slabs, one in front and one in the back of the UV and Ly $\alpha$  source. While the velocity and the other parameters of the approaching foreground slab are fixed by the observations (cf. Table 1), the velocity  $V_{\text{back}}$  of the receding slab is kept as a free parameter.

A good fit to the observed spectrum of cB58 is found for  $V_{\text{back}} \sim 140 \text{ km s}^{-1}$ , as shown in Fig. 6. For this choice of  $V_{\text{back}}$  the velocity shift of the receding slab is sufficient to allow a non-zero transmission of the reflected Ly $\alpha$  photons through the

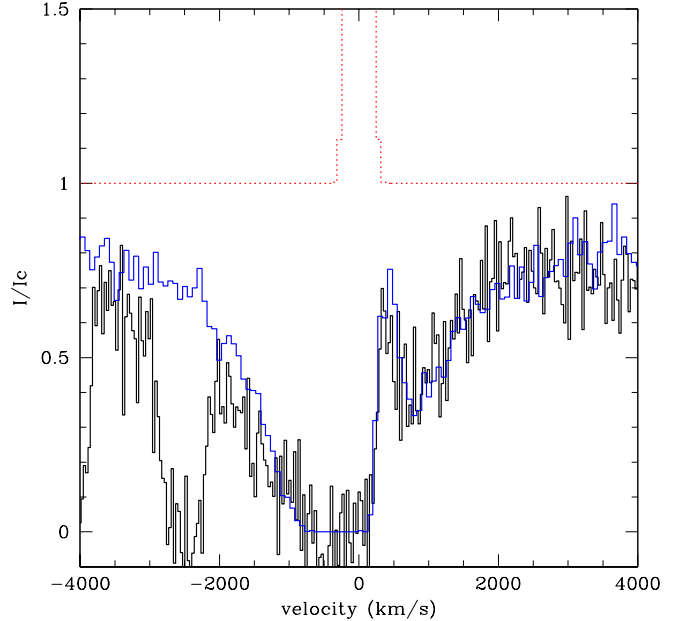


**Fig. 6.** Observed (black) and predicted Ly $\alpha$  line profile for the two slab model described in Sect. 4.3 (blue). The input spectrum is shown by the red dotted line.

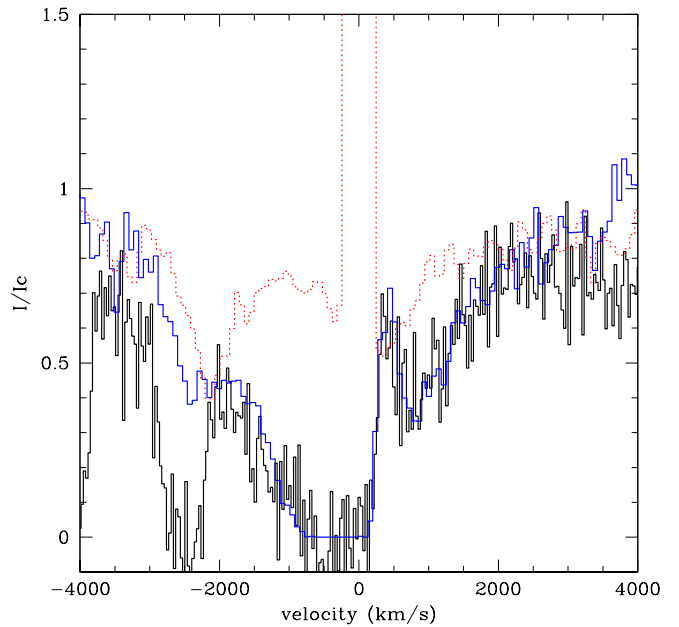


**Fig. 7.** Same as Fig. 6 but using high resolution spectra from evolutionary synthesis models for the description of the stellar continuum. The input spectrum, arbitrarily normalised, is shown by the red dotted line.

foreground slab, and low enough to produce the peak at the observed velocity of  $\sim 300 \text{ km s}^{-1}$ . The emergent spectrum is basically independent on the properties (e.g.  $N_{\text{H}}$ ) of the background slab, which merely acts as a moving mirror. This is clear since the spectrum reflected from a slab depends only on the thermal width  $b$ , and only weakly so ( $\propto b^{-1/2}$ ), as e.g. shown by Hansen and Oh (2006).

<sup>1</sup> As pointed out by Pettini et al. (2002) this possible small reshift could well be due to uncertainties in the absolute wavelength calibration.



Interestingly the value of the second free parameter, the intrinsic Ly $\alpha$  equivalent width  $EW(Ly\alpha)$ , is required to be  $EW \geq 80 \text{ \AA}$  to reproduce the observed strength of the Ly $\alpha$  emission peak. In our two slab model the solid angle under which the receding “mirror” is seen by the foreground slab governs the required EW, since this controls the relative amount of photons received from direct and reflected radiation at the back of the foreground slab. The lower limit on  $EW(Ly\alpha)$  given above is obtained by assuming a solid angle of  $2\pi$ . The observations are compatible with arbitrarily larger values of  $EW(Ly\alpha)$ .

Instead of the flat continuum we have also examined models using the more realistic synthetic spectra including stellar Ly $\alpha$  absorption presented above (Sect. 3.2.2) plus nebular Ly $\alpha$  emission as input for the radiation transfer calculations. The resulting Ly $\alpha$  profile, shown in Fig. 7, is of similar quality for a slightly lower input Ly $\alpha$  equivalent width of  $\geq 60 \text{ \AA}$ .

Fits using different combinations of the column density and extinction could be examined, given the uncertainty on the dust optical depth discussed above (cf. Sect. 2). Using e.g. lower values of  $E_g(B - V)$  and our “standard” value for  $N_H$  leads to a narrower Ly $\alpha$  absorption profile, which would require a higher column density. Quantifying the degeneracies around the solution found here is beyond the scope of this paper. In any case, it is quite clear that the main conclusion, a high column density and the need for a large intrinsic Ly $\alpha$  equivalent width, must be quite robust with respect to these degeneracies. This must be the case since a high column density is required to create the broad Ly $\alpha$  absorption (independently of the exact geometry), and in this case the escape fraction of Ly $\alpha$  photons “injected” close to line center is low quite independently of the exact dust content.

In summary, we conclude that with the simple geometry considered here we are able to reproduce for the first time the observed Ly $\alpha$  profile of cB58 with a radiation transfer model using all observed constraints on the outflow plus just two free parameters,  $V_{\text{back}}$  and  $EW(Ly\alpha)$ . One of the interesting conclusions from this analysis is to show that the observed absorption dominated Ly $\alpha$  line profile of cB58 is compatible with an intrinsically very different spectrum with a strong ( $EW(Ly\alpha) \geq 60 \text{ \AA}$ ) Ly $\alpha$  emission line. Radiation transfer effects and the presence of dust transform the intrinsic starburst spectrum to the observed one.

## 5. Discussion: a unifying scenario for Ly $\alpha$ emission in LBGs

As we have shown above the observed Ly $\alpha$  spectrum of cB58 is compatible with an *intrinsically* strong Ly $\alpha$  emission (with  $EW(Ly\alpha) > 60 \text{ \AA}$ ). Hence this is compatible with the equivalent width expected for a starburst with a constant star formation rate over  $> 50\text{--}100 \text{ Myr}$ , the timescale over which  $EW(Ly\alpha)$  reaches a constant equilibrium value of  $\sim 60\text{--}80 \text{ \AA}$  for a “standard” IMF and metallicities comparable to that of cB58 (see Fig. 3 and Schaerer 2003). Therefore the observed Ly $\alpha$  strength and profile are compatible with the star-formation histories derived from detailed modeling of the rest-UV properties, who consistently found a constant star formation rate and ages up to ages of  $\sim 20\text{--}100 \text{ Myr}$  (cf. de Mello et al. 2000; Ellingson et al. 1996; Pettini et al. 2000). Constant star formation over such timescales, instead of an aged burst which would be responsible for a low  $EW(Ly\alpha)$ , is also physically more plausible for objects like cB58 having large star formation rates, large physical scales, etc. Taking into account Ly $\alpha$  radiation transfer and dust allows us to reconcile these diagnostics.

Both detailed analysis of the rest-UV spectra of some LBGs and broad band SED fitting of many LBGs yields typically stellar ages of several hundred Myr and fairly constant or slowly decreasing star formation rates (cf. Papovich et al. 2001; Pentericci et al. 2007; Shapley et al. 2001). These results and our analysis of cB58 indicate fairly long star formation timescales, in contrast e.g. to the suggestion of Ferrara and Ricotti (2006).

cB58 is part of the quartile of  $z \sim 3$  LBGs showing a Ly $\alpha$  dominated by absorption with faint or little Ly $\alpha$  emission (Shapley et al. 2003). Therefore we can expect that these objects behave in a similar way as cB58 and hence have much higher *intrinsic* Ly $\alpha$  equivalent widths and higher *intrinsic* Ly $\alpha$  luminosities. In other words observed distribution functions of  $EW(Ly\alpha)$  and the Ly $\alpha$  luminosity function must be strongly modified by radiation transfer and dust effects, and the fraction of objects with low  $EW(Ly\alpha)$  ( $L(Ly\alpha)$ ) must be “artificially” overestimated.

Taking radiation transfer and dust into account, should therefore allow to reconcile observed Ly $\alpha$  strengths with relatively long ( $\gg 50 \text{ Myr}$ ) “duty cycles” of LBGs. In any case, age differences between  $\sim 200$  and  $400 \text{ Myr}$  found by Pentericci et al. (2007) for LBGs with and without Ly $\alpha$  emission respectively, cannot be the direct cause of the observed Ly $\alpha$  differences. If our scenario also works for Ly $\alpha$  emitters (henceforth LAEs, i.e. Ly $\alpha$  selected LBGs) and the suppression of Ly $\alpha$  photons is sufficient, it could explain the relatively low percentage of star-forming galaxies with no/little Ly $\alpha$  emission and hence reduce the need for short starburst episodes invoked e.g. by Malhotra and Rhoads (2002). This would then also help to reconcile the lower number densities of LAEs compared to LBGs despite the agreement in their bias (Kovač et al. 2007),

It may be reasonable to expect that most of the LBGs have quite very similar *minimum intrinsic* Ly $\alpha$  equivalent widths of  $\sim 60\text{--}80 \text{ \AA}$  determined by constant star formation over  $> 50\text{--}100 \text{ Myr}$ . Larger EWs are expected for objects dominated by younger ( $\leq 10\text{--}40 \text{ Myr}$ ) populations (cf. Fig. 3). Lower EWs would then be expected either in post-starburst objects or due to transfer and dust effects. Since the outflow velocities of LBGs do not vary strongly between subsamples with different Ly $\alpha$  strengths<sup>2</sup> we propose that the main factor leading to the diversity of Ly $\alpha$  strengths in LBGs is their  $H \text{ I}$  column density and concomitantly their dust content<sup>3</sup>.

This suggestion is compatible with the observational correlations found between  $E(B-V)$  and  $EW(Ly\alpha)$  (e.g. Shapley et al. 2003; Tapken et al. 2007) and with the differences in extinction found by Pentericci et al. (2007) between two subsamples of  $z \sim 4$  LBGs. It also broadly agrees with Ly $\alpha$  line profile fitting of LBGs with strong Ly $\alpha$  emission, discussed in the next paper of this series (Verhamme et al. 2007).

Given observed mass-metallicity relations (e.g. Erb et al. 2006; Tremonti et al. 2004) it may be quite natural to speculate that the difference in  $N_H$  and dust content is related to the galaxy mass to first order. The data of Shapley et al. (2001) show such a trend. In this case more massive LBGs would be more dusty, and hence show lower  $EW(Ly\alpha)$ , although they could have identical Ly $\alpha$  emission properties intrinsically. Such a trend is e.g. found by Pentericci et al. (2007). The absence of bright LBGs (in the

<sup>2</sup> The expansion velocities determined by one third of the velocity shift between the interstellar absorption lines and the Ly $\alpha$  peak,  $V_{\text{exp}} \sim 1/3\Delta(V_{\text{ISM}}, V(Ly\alpha))$  is  $\sim 160\text{--}260 \text{ km s}^{-1}$  for the sample of Shapley et al. (2003).

<sup>3</sup> If the dust-to-gas ratio remains constant, both  $N_H$  and the dust content increase in lockstep.

UV restframe) with high Ly $\alpha$  equivalent widths (in emission) reported in many papers (e.g. Ando et al. 2004; Shapley et al. 2003; Tapken et al. 2007) would also naturally be explained by this fact, if the SFR correlates with mass, as observed for star forming galaxies out to  $z \sim 2$  (see Daddi et al. 2007; Elbaz et al. 2007; Noeske et al. 2007).

Relevant for determining the Ly $\alpha$  properties are however, the total H I column density and the relative dust to H I content. Assuming the latter to be constant<sup>4</sup>, the above suggestion would imply larger amounts of H I in more massive LBGs, known to hold at least in nearby galaxies (Kennicutt 1998). However, since the H I responsible for shaping Ly $\alpha$  is found in outflows it may only trace a fraction of the total neutral hydrogen content. Hence the H I column density derived from the Ly $\alpha$  fits may not be a good tracer of the gas mass, and hence may not simply scale with galaxy mass. Correlating the outflow properties more closely to those of the host galaxy may require dynamical modeling (e.g. Blaizot and et al. 2007; Ferrara and Ricotti 2006).

While the “scenario” proposed here to explain the diversity of Ly $\alpha$  line strengths in LBGs seems consistent with the observations, it remains to be tested more generally. LBGs with strong Ly $\alpha$  emission have also been studied with our radiation transfer models for this purpose and are broadly in agreement with the scenario proposed here (Verhamme et al. 2007). Alternative explanations have also been proposed. For example Shapley et al. (2001) have from empirical evidence suggested age as the main difference in LBGs, where younger objects are more dusty, and hence show less Ly $\alpha$  emission. However, it is not clear why older LBGs would contain less dust, especially since outflows, supposedly used to expel the dust, are ubiquitous in all LBGs and since precisely these outflows are the location where the emergent Ly $\alpha$  spectrum is determined. Also, why would younger LBGs be more massive than older ones as their data would imply? Ferrara and Ricotti (2006) have proposed that LBGs host short-lived ( $30 \pm 5$  Myr) starburst episodes, whose outflows – when observed at different evolutionary phases – would give rise to the observed correlations between IS lines and Ly $\alpha$ . However, their conclusion may need to be revised since the “observed” wind velocity versus SFR relation (their Fig. 1) is incorrect and flatter than assumed<sup>5</sup>. Furthermore the ages obtained from SED and spectral fits of LBGs show older ages and fairly constant star formation histories, as already mentioned earlier.

In paper III of this series (Verhamme et al. 2007) we will examine how our models are able to explain various correlations observed among Ly $\alpha$ , IS lines, and other properties of LBGs (Shapley et al. 2003) and LAEs. Further work will be needed to test the scenario proposed here, to understand more precisely the relations between LBGs and LAEs, and to understand the links between star-formation, host galaxy, and outflow properties.

## 6. Conclusions

A 3D Ly $\alpha$  and UV continuum radiation transfer code (Verhamme et al. 2006) has for the first time been applied to the

<sup>4</sup> Combining e.g. the dependence of the dust-to-gas ratio on metallicity O/H from Lisenfeld and Ferrara (1998) with the mass-metallicity relation at  $z \gtrsim 2$  (Erb et al. 2006), gives a very small dependence of the dust-to-gas ratio on galaxian mass.

<sup>5</sup> They assume  $v_w = 1/2\Delta(V_{\text{ISM}}, V(\text{Ly}\alpha))$  instead of the weaker dependence  $v_w \sim 1/3\Delta(V_{\text{ISM}}, V(\text{Ly}\alpha))$  obtained from shell models and supported by direct measurements of stellar, IS, and Ly $\alpha$  velocity shifts. Furthermore their SFR values differ from those quoted in Shapley et al. (2003).

prototypical Lyman break galaxy MS 1512–cB58 at  $z = 2.7$ . Since this is one of, if not the best studied LBG, and since it is part of the quartile of LBGs showing predominantly Ly $\alpha$  in absorption (cf. Shapley et al. 2003), a detailed Ly $\alpha$  line profile analysis including radiation transfer and dust effects is of great interest.

Three different geometries were explored for the material surrounding the central starburst; a spherically symmetric expanding shell with velocity  $V_{\text{exp}}$ , a foreground slab moving towards the observer, and a geometry mimicing a shell with a lower velocity in the back. All available observational constraints were used (see Table 1). In particular these include: the velocity  $V_{\text{exp}}$  of the foreground material, its Doppler parameter  $b$ , column density  $N_{\text{H}}$ , and the observed extinction. The width of the intrinsic Ly $\alpha$  emission was taken from the observed FWHM of H $\alpha$ . The two free parameters were: the equivalent width of the intrinsic Ly $\alpha$  emission, and the velocity  $V_{\text{back}}$  of the background slab (if applicable).

Our radiation transfer calculations have confirmed what could be expected from our earlier expanding shell simulations and from the lower-than-usual observed velocity shift between the peak of “remnant” Ly $\alpha$  emission and the blue IS absorption lines (cf. Sect. 2.1); the Ly $\alpha$  line profile of cB58 cannot be reproduced by an expanding shell with isotropic constant velocity  $V_{\text{exp}}$ . Considering, however, a lower shell velocity in the back allowed us to obtain excellent fits to the observed Ly $\alpha$  line profile. Interestingly, the input spectrum requires a fairly strong Ly $\alpha$  emission, with a lower limit of  $\text{EW}(\text{Ly}\alpha) \gtrsim 60 \text{ \AA}$ . Radiation transfer and the suppression of photons by dust are responsible for transforming such an input spectrum into the observed Ly $\alpha$  absorption profile with a superposed faint emission peak. In this way the observed Ly $\alpha$  line strength and profile can be reconciled with the strong intrinsic Ly $\alpha$  emission expected from the approximately constant star-formation history of cB58 derived from earlier detailed UV spectral analysis (cf. de Mello et al. 2000; Pettini et al. 2000).

In fact we suggest that cB58 and most other LBGs have intrinsically  $\text{EW}(\text{Ly}\alpha) \sim 60\text{--}80 \text{ \AA}$  or larger, and that the main physical parameter responsible for the observed variety of Ly $\alpha$  strengths and profiles in LBGs is  $N_{\text{H}}$  and the accompanying variation of the dust content (see Sect. 5). This explains not only the absorption-dominated object cB58, but also observed correlations between E(B-V) and  $\text{EW}(\text{Ly}\alpha)$  in LBGs, the absence of bright LBGs with strong Ly $\alpha$  emission, and other correlations.

Among the implications from our work are that observed  $\text{EW}(\text{Ly}\alpha)$  distributions and Ly $\alpha$  luminosity functions must be corrected for radiation transfer and dust effects. Furthermore relatively short duty cycles, suggested earlier in the literature, are not required to explain the variations observed between different LBG types. Our proposed unifying scenario will be detailed further and subjected to additional tests in a subsequent publication on a sample of LBGs with strong Ly $\alpha$  emission (Verhamme et al. 2007). Providing a clearer picture of the physical links between the observables including Ly $\alpha$  line strength and profile, and the star-formation, host galaxy, and outflow properties and evolution of LBGs and LAEs remains an objective for the near future.

*Acknowledgements.* We thank Max Pettini and Sandra Savaglio for providing us with their high resolution UV spectra of cB58, and Miguel Cerviño for synthetic high-resolution spectra. This work was supported by the Swiss National Science Foundation.

## References

Ando, M., Ohta, K., Iwata, I., Watanabe, C., Tamura, N., Akiyama, M., and Aoki,



- K.: 2004, *ApJ* **610**, 635
- Baker, A. J., Lutz, D., Genzel, R., Tacconi, L. J., and Lehnert, M. D.: 2001, *A&A* **372**, L37
- Baker, A. J., Tacconi, L. J., Genzel, R., Lehnert, M. D., and Lutz, D.: 2004, *ApJ* **604**, 125
- Bechtold, J., Yee, H. K. C., Elston, R., and Ellingson, E.: 1997, *ApJL* **477**, L29+
- Blaizot, J. and et al.: 2007, *A&A* in preparation
- Calzetti, D., Armus, L., Bohlin, R. C., Kinney, A. L., Koornneef, J., and Storchi-Bergmann, T.: 2000, *ApJ* **533**, 682
- Charlot, S. and Fall, S. M.: 1993, *ApJ* **415**, 580
- Daddi, E., Dickinson, M., Morrison, G., Chary, R., Cimatti, A., Elbaz, D., Frayer, D., Renzini, A., Pope, A., Alexander, D. M., Bauer, F. E., Giavalisco, M., Huynh, M., Kurk, J., and Mignoli, M.: 2007, *ApJ* **670**, 156
- de Mello, D. F., Leitherer, C., and Heckman, T. M.: 2000, *ApJ* **530**, 251
- Delgado, R. M. G., Cerviño, M., Martins, L. P., Leitherer, C., and Hauschildt, P. H.: 2005, *MNRAS* **357**, 945
- Elbaz, D., Daddi, E., Le Borgne, D., Dickinson, M., Alexander, D. M., Chary, R.-R., Starck, J.-L., Brandt, W. N., Kitzbichler, M., MacDonald, E., Nonino, M., Popesso, P., Stern, D., and Vanzella, E.: 2007, *A&A* **468**, 33
- Ellingson, E., Yee, H. K. C., Bechtold, J., and Elston, R.: 1996, *ApJL* **466**, L71
- Erb, D. K., Shapley, A. E., Pettini, M., Steidel, C. C., Reddy, N. A., and Adelberger, K. L.: 2006, *ApJ* **644**, 813
- Ferrara, A. and Ricotti, M.: 2006, *MNRAS* **373**, 571
- Frayer, D. T., Papadopoulos, P. P., Bechtold, J., Seaquist, E. R., Yee, H. K. C., and Scoville, N. Z.: 1997, *AJ* **113**, 562
- Hansen, M. and Oh, S. P.: 2006, *MNRAS* **367**, 979
- Heckman, T. M., Sembach, K. R., Meurer, G. R., Leitherer, C., Calzetti, D., and Martin, C. L.: 2001, *ApJ* **558**, 56
- Kennicutt, Jr., R. C.: 1998, *ARA&A* **36**, 189
- Kovač, K., Somerville, R. S., Rhoads, J. E., Malhotra, S., and Wang, J.: 2007, *ApJ* **668**, 15
- Lanz, T. and Hubeny, I.: 2003, *ApJS* **146**, 417
- Leitherer, C.: 2007, In *"Ly- $\alpha$  workshop: lessons from local to high- $z$  galaxies"* IAP, Paris, [www2.iap.fr/lyman07/](http://www2.iap.fr/lyman07/)
- Leitherer, C., Robert, C., and Heckman, T. M.: 1995, *ApJS* **99**, 173
- Leitherer, C., Schaerer, D., Goldader, J. D., Delgado, R. M. G., Robert, C., Kune, D. F., de Mello, D. F., Devost, D., and Heckman, T. M.: 1999, *ApJS* **123**, 3
- Lisenfeld, U. and Ferrara, A.: 1998, *ApJ* **496**, 145
- Malhotra, S. and Rhoads, J. E.: 2002, *ApJL* **565**, L71
- Martins, F.: 2000, *Master's thesis*, Université Paul-Sabatier, Toulouse
- Nakanishi, K., Ohta, K., Takeuchi, T. T., Akiyama, M., Yamada, T., and Shioya, Y.: 1997, *PASJ* **49**, 535
- Noeske, K. G., Weiner, B. J., Faber, S. M., Papovich, C., Koo, D. C., Somerville, R. S., Bundy, K., Conselice, C. J., Newman, J. A., Schiminovich, D., Le Floch, E., Coil, A. L., Rieke, G. H., Lotz, J. M., Primack, J. R., Barmby, P., Cooper, M. C., Davis, M., Ellis, R. S., Fazio, G. G., Guhathakurta, P., Huang, J., Kassin, S. A., Martin, D. C., Phillips, A. C., Rich, R. M., Small, T. A., Willmer, C. N. A., and Wilson, G.: 2007, *ApJL* **660**, L43
- Papovich, C., Dickinson, M., and Ferguson, H. C.: 2001, *ApJ* **559**, 620
- Pentericci, L., Grazian, A., Fontana, A., Salimbeni, S., Santini, P., de Santis, C., Gallozzi, S., and Giallongo, E.: 2007, *A&A* **471**, 433
- Pettini, M., Rix, S. A., Steidel, C. C., Adelberger, K. L., Hunt, M. P., and Shapley, A. E.: 2002, *ApJ* **569**, 742
- Pettini, M., Steidel, C. C., Adelberger, K. L., Dickinson, M., and Giavalisco, M.: 2000, *ApJ* **528**, 96
- Savaglio, S., Panagia, N., and Padovani, P.: 2002, *ApJ* **567**, 702
- Sawicki, M.: 2001, *AJ* **121**, 2405
- Schaerer, D.: 2003, *A&A* **397**, 527
- Seaton, M. J.: 1979, *MNRAS* **187**, 73P
- Seitz, S., Saglia, R. P., Bender, R., Hopp, U., Belloni, P., and Ziegler, B.: 1998, *MNRAS* **298**, 945
- Shapley, A. E., Steidel, C. C., Adelberger, K. L., Dickinson, M., Giavalisco, M., and Pettini, M.: 2001, *ApJ* **562**, 95
- Shapley, A. E., Steidel, C. C., Pettini, M., and Adelberger, K. L.: 2003, *ApJ* **588**, 65
- Tapken, C., Appenzeller, I., Noll, S., Richling, S., Heidt, J., Meinköhn, E., and Mehlert, D.: 2007, *A&A* **467**, 63
- Teplitz, H. I., Malkan, M. A., and McLean, I. S.: 2004, *ApJ* **608**, 36
- Teplitz, H. I., McLean, I. S., Becklin, E. E., Figer, D. F., Gilbert, A. M., Graham, J. R., Larkin, J. E., Levenson, N. A., and Wilcox, M. K.: 2000, *ApJL* **533**, L65
- Tremonti, C. A., Heckman, T. M., Kauffmann, G., Brinchmann, J., Charlot, S., White, S. D. M., Seibert, M., Peng, E. W., Schlegel, D. J., Uomoto, A., Fukugita, M., and Brinkmann, J.: 2004, *ApJ* **613**, 898
- Valls-Gabaud, D.: 1993, *ApJ* **419**, 7
- Verhamme, A., Schaerer, D., Atek, H., and Tapken, C.: 2007, *A&A* in preparation
- Verhamme, A., Schaerer, D., and Maselli, A.: 2006, *A&A* **460**, 397
- Yee, H. K. C., Ellingson, E., Bechtold, J., Carlberg, R. G., and Cuillandre, J.-C.: